CALCIUM SENSORS ALG-2 AND PEFLIN BIND ER EXIT SITES IN ALTERNATE STATES TO MODULATE SECRETION IN RESPONSE TO CALCIUM SIGNALING

John Sargeant[1], Tucker Costain[1], Corina Madreiter-Sokolowski[2], David E. Gordon[3], Andrew A. Peden[4], Roland Mali[5], Wolfgang F. Graier[5], and Jesse C. Hay[1]

[1]Division of Biological Sciences, Center for Structural & Functional Neuroscience, University of Montana, USA; [2]Department of Health Sciences and Technology, ETH Zürich, Switzerland; [3]Cellular and Molecular Pharmacology, University of California, San Francisco, USA; [4]Department of Biomedical Science & Centre for Membrane Interactions and Dynamics, The University of Sheffield, United Kingdom; [5]Molecular Biology and Biochemistry, Gottfried Schatz Research Center, Medical University of Graz, Austria

correspondence: jesse.hay@umontana.edu

ABSTRACT

Penta EF-hand (PEF) proteins apoptosis-linked gene 2 (ALG-2) and peflin are cytoplasmic Ca^{2+} sensors for which physiological roles are still emerging. Here we demonstrate that adjustment of the ALG-2:peflin expression ratio can modulate basal ER export rates up or down by 107% of the basal rate. Through their ALG-2 subunit, ALG-2-peflin hetero-oligomers are shown to bind ERES and inhibit ER export of multiple cargo types, including collagen I, while ALG-2 by itself binds ERES to stimulate cargo sorting and ER export. During sustained Ca^{2+} signaling, peflin and ALG-2 are demonstrated to sharply lower ER export rates by 40% in a novel secretory response to demanding physiological conditions. However, in highly Ca^{2+}-stressed cells, peflin's suppressive role appears to promote pro-apoptotic unfolded protein response (UPR) signaling, indicating that the regulation is not necessarily pro-survival. Thus, regulation of secretion by PEF protein sub-complex binding to ERES in response to Ca^{2+} signals impacts key cellular decision processes relevant to aging, neurodegeneration and diabetes.

INTRODUCTION

The ER-to-Golgi interface is the busiest vesicle trafficking step, transporting up to one-third

of all eukaryotic proteins (Ghaemmaghami *et al.*, 2003). Anterograde cargo is captured into a COPII pre-budding complex containing the inner coat sec23/24 heterodimer, which binds cargo in several distinct pockets on the membrane-proximal surface of sec24 (Bi *et al.*, 2007; Hughes and Stephens, 2008; Stagg *et al.*, 2008; Miller and Barlowe, 2010). Recruitment of the outer coat layer, comprised of sec13/31, positions a flexible proline rich region (PRR) loop of sec31 across the membrane-distal surface of sec23, potentiating its Sar1 GAP activity required for cargo concentration (Tabata *et al.*, 2009). Sec13/31 recruitment involves polymerization of at least 24 heterotetramers (Stagg *et al.*, 2008).

Regulatory roles for Ca^{2+} in intracellular membrane fusions are still becoming clear. Recent work on ER-to-Golgi transport demonstrates that this step requires luminal Ca^{2+} stores at a stage following cargo biogenesis and folding/assembly, perhaps through release of Ca^{2+} into the cytoplasm where it binds and activates the vesicle budding, docking and/or fusion machinery (Bentley *et al.*, 2010; Helm *et al.*, 2014). Depletion of luminal calcium with ER Ca^{2+} ATPase (SERCA) inhibitors leads to significantly reduced transport and a buildup of budding and newly budded COPII vesicles and vesicle proteins (Bentley *et al.*, 2010; Helm *et al.*, 2014). Effector mechanisms by which Ca^{2+} modulates ER-to-Golgi transport appear to involve penta-EF-hand-containing (PEF) protein adaptors that have been implicated in many Ca^{2+}-dependent cellular phenomena (Maki *et al.*, 2002). The PEF protein apoptosis-linked gene-2 (ALG-2) acts as a Ca^{2+} sensor at ER exit sites and stabilizes association of sec31 with the membrane when Ca^{2+} is present (Yamasaki *et al.*, 2006; la Cour *et al.*, 2007; Shibata *et al.*, 2007; 2010). Most ALG-2 in cell extracts exists in a stable heterodimer with the PEF protein peflin that binds ALG-2 in a Ca^{2+}-inhibited manner (Kitaura *et al.*, 2001; 2002) and has been shown to suppress ER export of the cargo marker VSVG-GFP, perhaps by modulating ALG-2 availability to bind ERES (Rayl *et al.*, 2016). Despite all of these observations, a unified model for when and how PEF proteins modulate secretion has not emerged. For example, most in vitro transport reconstitutions and results with purified ALG-2 have indicated that the protein is an inhibitor of vesicle budding or fusion (Bentley *et al.*, 2010; la Cour *et al.*, 2013). On the other hand some recent intact cell trafficking experiments indicate a suppressive role for ALG-2 based upon ALG-2 depletion (Shibata *et al.*, 2015), while we implied a stimulatory role for ALG-2 because peflin suppressed transport by antagonizing stimulatory ALG-2-Sec31A interactions (Rayl *et al.*, 2016). Furthermore, work on a presumed ALG-2 ortholog in yeast, Pef1p, demonstrated an inverse

relationship, wherein Pef1p binding to the sec31 PRR was *inhibited* by Ca^{2+} and delayed coat recruitment to the membrane (Yoshibori *et al.*, 2012).

Here we advance understanding of PEF protein secretory regulation by demonstrating that ALG-2 binding to ERES can *either* inhibit *or* stimulate ER-to-Golgi transport, depending upon whether it exists as a peflin-ALG-2 hetero-oligomeric complex--acting as an inhibitor, or in a peflin-lacking ALG-2 species--acting as an accelerator. The basal secretion rate can thus be modulated up and down depending upon ALG-2:peflin expression ratios or by Ca^{2+} signals that alter the sub-complex ratios. Furthermore, during agonist-driven Ca^{2+} signaling for an hour or more, ALG-2 and peflin dynamics result in a significant reduction of the biosynthetic secretion rate, presumably to adapt the secretory pathway to potential Ca^{2+} stress. Many adaptive responses can become maladaptive during extreme stress. In this light, we report that in highly Ca^{2+}-stressed cells, peflin contributes significantly to pro-apoptotic UPR signaling.

RESULTS

Expression ratios of ALG-2 and peflin define the dynamic range over which they regulate ER-to-Golgi transport

To investigate the dynamic range and functional interactions of PEF protein regulation of ER export, we forced individual, tandem, or reciprocal expression changes of the two proteins. Endogenous peflin and ALG-2 were either knocked down using transfection with siRNA or over-expressed by transfection with the wt, untagged rodent proteins in NRK cells. After 48 hours of transfection, the initial rate of ER-to-Golgi transport of the synchronizeable cargo transmembrane protein VSV-G_{ts045}-GFP was determined by incubation for 10 minutes at the permissive temperature followed immediately by fixation and morphological quantitation of the ratio of VSV-G that has reached the Golgi vs. remaining in the ER, as before (Rayl *et al.*, 2016). Figure 1 columns 1 and 2 show that as previously reported (Rayl *et al.*, 2016), peflin knockdown in the presence of normal levels of ALG-2 significantly increased VGV-G transport above basal by ~84%. On the other hand, over-expression of peflin (column 3) decreased transport by 23% below basal. Interestingly, the same two manipulations of ALG-2 expression in the presence of normal levels of peflin (columns 4 and 5) caused much less change in transport, indicating that at steady state, peflin expression levels are bi-directionally rate-limiting for secretion, but ALG-2 expression levels are much less

impactful. Forced peflin over- and under-expression thus defines a dynamic range of PEF protein regulation of transport at about 107% of basal secretory flux (84% above basal and 23% below).

We next asked whether the effects of peflin over- and under-expression depended upon the presence of ALG-2. As shown in Figure 1 columns 6 and 7, in the absence of ALG-2 expression, forced changes in peflin expression change secretion by only 20%, indicating that peflin is dependent upon ALG-2 to influence transport. This suggests that peflin's proximal target is ALG-2, which in turn binds sec31A to influence transport. Interestingly, column 6 also indicates that in the absence of both ALG-2 and peflin, secretion is higher than in the presence of both proteins at normal levels. This demonstrates that these PEF proteins are not required for transport, and suggests that the two of them together exert a slightly suppressive effect on ER-to-Golgi transport under steady-state conditions. In sum, varying PEF protein expression ratios provide cells the opportunity to modulate secretion significantly in both directions.

ALG-2 and peflin bind ERES in multiple states that affect transport differently

Since the subcellular distribution of peflin was largely unknown, we raised a rabbit polyclonal antibody against rat peflin to be used for localization studies of the endogenous protein. We also produced a chicken polyclonal antibody against mouse ALG-2 to be used in co-localization studies with peflin. Although peflin was previously thought to be a soluble cytoplasmic protein, we observed diffuse cytosolic as well as a distinctly punctate localization for peflin throughout the cytoplasm. In addition, endogenous peflin was not only present but significantly concentrated in the nucleus (Figure 2C, upper right). The diffuse and punctate cytoplasmic, as well as nuclear labeling was specific for endogenous peflin since peflin siRNA transfection reduced all three types of labeling (Figure 2C, right, second from bottom). Peflin cytosolic puncta noticeably co-localized with the ALG-2 cytosolic puncta previously identified as ER exit sites (ERES) (Yamasaki *et al.*, 2006; la Cour *et al.*, 2007; Shibata *et al.*, 2007), in these experiments also marked by GFP-sec13. Co-localization of endogenous peflin and ALG-2 at ERES was an unexpected result, since previous research focused on peflin/ALG-2 heterodimers as a soluble species (Kitaura *et al.*, 2001) and interactions with peflin seemed to keep ALG-2 away from ERES (Rayl *et al.*, 2016). We found that 95% of ERES defined by GFP-sec13 were positive for ALG-2 and that the vast majority of ERES (>75%) were positive for both ALG-2

and peflin (supplemental Figure 1). To determine the interdependence of peflin and ALG-2 for localization at ERES, we manipulated their expression levels as in Figure 1 and then quantified the labeling intensity of the two proteins specifically at ERES as defined by the GFP-sec13 marker. Knockdown of ALG-2 removed peflin from ERES, implying that peflin was dependent on ALG-2 for targeting to ERES (not shown). Furthermore, in the absence of ALG-2, over-expression of peflin did not restore it to ERES (Figure 2A, bars 1 and 2), though peflin over-expression greatly increased peflin at ERES in the presence of ALG-2 (Figure 2A, bar 4). ALG-2 targeting to ERES, on the other hand, did not depend upon, but was negatively influenced by peflin. Peflin depletion greatly enhanced ALG-2 targeting to ERES (Figure 2B, bars 1 vs. 3), and peflin over-expression reduced it (Figure 2B bars 1 vs. 4).

The targeting data indicates that peflin binds ERES through ALG-2 as part of an ALG-2-peflin complex, most likely the heterodimer species previously described (Kitaura *et al.*, 2001). However, since removal of peflin increases ALG-2 binding, ALG-2 must also bind in other states, perhaps the previously described homo-dimer (Takahashi *et al.*, 2015). Importantly, the high secretion caused by the lack of peflin and the low secretion caused by excess peflin are approximately equally above and below, respectively, the secretion in the absence of either protein (Figure 1); this demonstrates that cytosolic peflin does not simply act as an ALG-2 sink or sponge that inhibits transport by withdrawing stimulatory ALG-2 from ERES. Rather, peflin-containing ALG-2 species must exert an inhibitory influence on transport, while peflin-lacking ALG-2 species must exert a stimulatory influence. In summary, peflin-ALG-2 complexes bind ERES and inhibit ER export, while ALG-2 by itself binds ERES to stimulate export.

ALG-2/peflin complexes affect ER export similarly for multiple actively-secreted cargos

A recent study reported that in a chondrocyte cell line, peflin depletion inhibited ER-to-Golgi transport of collagen I, implying that peflin was *required* for collagen export from the ER (McGourty *et al.*, 2016). Since our results have instead suggested a *suppressive* role for peflin in VSV-G export, we investigated whether peflin may have opposite effects on different actively sorted cargoes. To address this, we expressed different cargoes in NRK cells and tested the effects of peflin depletion. As seen if Figure 3A, compared to VSV-G-GFP, export of GFP-collagen I was even more strongly stimulated by peflin depletion (bars 1 and 2 vs.3 and 4), supporting a suppressive effect of peflin under normal conditions. Since both VSV-G_{ts045}-GFP

and collagen export were synchronized by incubation at a restrictive temperature followed by a shift to permissive temperature, we wanted to rule out that the temperature shift was involved in the suppressive effects of peflin. We created novel reporter constructs containing a conditional aggregation domain, F_M4, that aggregates in the ER and prevents export until a small molecule drug, AP21998, is provided (Rivera *et al.*, 2000), causing synchronous ER export. The first construct included GFP as a luminal domain followed by FM4 and then the VSV-G transmembrane domain as a membrane anchor and ER export signal (GFP-F_M4-$VSVG_{tm}$). The second construct was similar but included the GPI anchor from CD55 at the C-terminus instead of a transmembrane domain (GFP-F_M4-GPI). GPI anchors function as an export sequence recognized and sorted in a p24-dependent manner (Bonnon *et al.*, 2010). Both constructs, when triggered by ligand AP21998 were actively transported from the ER to the Golgi in 10 minutes, and for both constructs, peflin depletion caused a highly significant increase in ER-to-Golgi transport (Figure 3, bars 5-8). A third construct, GFP-F_M4-GH (Gordon *et al.*, 2010), was fully luminal, contained human growth hormone, and lacked any ER export sequence. Peflin depletions caused a significant decrease in ER export of this bulk flow construct, consistent with a recent study demonstrating that COPII sorting works in part by exclusion of proteins that are not actively included (Ma *et al.*, 2017). This result implies that peflin depletion does not act simply to accelerate vesicle production, but rather stimulates COPII function broadly--including its sorting function. In summary, Figure 3 establishes that the stimulatory effects of peflin depletion on transport are not restricted to high temperature-synchronized reporter cargoes, and that four actively sorted cargoes, VSV-G_{ts045}-GFP, GFP-collagen I, GFP-F_M4-$VSVG_{tm}$ and GFP-F_M4-GPI, containing three distinct ER export signals, are exported more efficiently in the absence of peflin in NRK cells.

NRK cells may not be an adequate model for ER-to-Golgi transport for certain cargoes, for example collagen I, which require specific cargo adaptors and modified vesicles for efficient export (Saito *et al.*, 2009; Wilson *et al.*, 2011; McCaughey *et al.*, 2016; Raote *et al.*, 2018). The vast majority of Collagen I is secreted by fibroblasts, osteoblasts and chondrocytes. To address whether peflin also suppressed secretion of collagen I in cells whose normal function is to secrete collagen I in abundance, we tested the effects of peflin depletion on endogenous collagen I secretion in Rat2 embryonic fibroblasts. Procollagen I folds inefficiently in the ER and mis-folded procollagen undergoes degradation by non-canonical autophagy at ERES (Omari *et al.*,

2018). To be certain that non-secretory collagen fates potentially affected by peflin expression did not interfere with our assay for ER-to-Golgi transport, we monitored total cell fluorescence (TCF) of endogenous collagen I in addition to the Golgi:ER intensity ratio that constitutes the ER-to-Golgi transport index. We measured ER-to-Golgi transport and collagen I TCF and in the same cells with and without peflin depletion, and found that peflin depletion increased the ER-to-Golgi transport index by 75% (Figure 4A) but had no significant effect on collagen I TCF (Figure 4B). Furthermore, as shown in Figure 4C, our method for measuring collagen I TCF was quantitative and reflected collagen I content since titration of cells with a collagen I-specific siRNA resulted in distinct, decreasing TCF values. Importantly, once again peflin depletion did not result in a significant change in TCF (Figure 4C, first and last columns). Together these data indicate that peflin depletion dramatically increases transport of endogenous collagen I from the ER to Golgi in fibroblasts, and does not affect collagen export from the ER for degradation.

ALG-2 activates a mechanism to sharply decrease ER export during Ca^{2+} agonist stimulation

Since peflin and ALG-2 are regulated by Ca^{2+} binding, we tested whether their ability to regulate ER-to-Golgi transport was affected by cytoplasmic Ca^{2+} signaling. Histamine receptors present on many cell types activate phospholipase C via G_Q to stimulate Ca^{2+} release by IP3 receptor channels on the ER. Figure 5A demonstrates that NRK cells respond to extracellular histamine application with intense cytoplasmic Ca^{2+} fluxes and periodic oscillations. Importantly, signaling can persist for at least 20 minutes without diminution or down-regulation of response, indicating that our model is appropriate for examination of both short- and long-term effects of Ca^{2+} release on ER export. As shown in Figure 5B (black circles), 10 minutes of ER-to-Golgi transport initiated after increasing times of exposure to histamine indicated that initially and for up to 30 minutes of exposure, no significant modulation of the transport rate occurred. However, by 60 minutes of exposure, ER-to-Golgi transport was significantly reduced, with continued reduction for up to 150 minutes, wherein transport was reduced by 40% below basal conditions. Thus, NRK epithelial cells respond to prolonged Ca^{2+} agonist exposure by sharply curtailing ER secretory output, a hitherto unknown physiological phenomenon, presumably for adaptation of the secretory pathway to stressful conditions and/or pathogen invasion.

We next tested the involvement of PEF proteins in the down-modulation. Significantly, the

Ca^{2+}-dependent modulation of transport was entirely dependent upon the presence of ALG-2, since knockdown of ALG-2 prevented any change in transport over the same timecourse (Figure 5B, green circles). The down-modulation, however, did not require peflin, since peflin knockdown did not prevent the decrease in ER-to-Golgi transport (Figure 5C, magenta circles), although in the absence of peflin ER export always remained above basal, control levels. This indicates that although peflin is not the trigger, it is required for the full suppressive effect. Furthermore, over-expression of peflin did not further suppress transport during Ca^{2+}-activated depression of ER export (Figure 5C, bars 3 and 4). This suggests that while peflin is still rate-limiting during the suppressed transport phase, it's suppressive effects may have been maximized. One possibility would be that the peflin:ALG-2 ratio had already been increased maximally during histamine exposure. Future work should examine the mechanism further.

Peflin regulates pro-apoptotic UPR signaling

We have shown that PEF proteins can regulate ER-to-Golgi transport rates through their expression ratios and through Ca^{2+}-dynamics. However, what is the advantage to cells to regulate basal ER-to-Golgi transport rates? Under what physiological conditions does the bipartite PEF regulatory system become rate-limiting and important for cell function and/or survival? To begin answering this question, we utilized porcine aortic endothelial cells (PAECs), primary cells that undergo cellular ageing and senescence after passaging five times (P5) in vitro. As recently demonstrated (Madreiter-Sokolowski *et al.*, 2019), P5 PAECs display ER Ca^{2+}-driven mitochondrial overload, oxidative stress, as well as profoundly increased UPR signaling and expression of CHOP, a UPR transcription factor involved in the transition from UPR to apoptosis. Under these Ca^{2+} stress conditions, we found by quantitative reverse-transcription PCR (qRT-PCR) that a 60% knockdown of peflin using siRNA resulted in a specific 45% reduction in expression of the UPR target gene GRP78, and a 55% reduction of CHOP (Figure 6). This demonstrates that peflin expression facilitates life-threatening stress in aging endothelial cells.

DISCUSSION

ALG-2 and peflin function at ERES at steady-state and intense signaling conditions

An important conclusion here is that ALG-2 serves as both an inhibitor and an accelerator of transport, depending upon its configuration at the ERES. When complexed as a putative homodimer bound to Sec31A, it acts as an accelerator, and when complexed with peflin as a putative heterodimer bound to Sec31A via ALG-2, it inhibits transport. This argument depends upon two findings from Figures 1 and 2: First, ALG-2 is the effector of peflin's actions; peflin can neither bind to ERES nor influence transport in the absence of ALG-2. Second, depletion of ALG-2 produces a level of transport, approximately 120% of control, that is roughly mid-way between the extremes of 190%, when peflin is knocked down, and 75%, when peflin is over-expressed. So, under steady-state and peflin-over-expression conditions, ALG-2 is suppressing transport, but in the absence of peflin it accelerates transport. Although ALG-2, but not peflin, is strictly required for the inhibition of transport under Ca^{2+} signaling conditions, our data does not distinguish whether this is due to loss of its stimulatory form vs. an increase of its inhibitory form, or both. However, since inhibition of transport in signaling requires ALG-2 to trigger the response and peflin to fully inhibit (Figure 5), our data favors loss of ALG-2's stimulatory action while maintaining its inhibitory action.

There are many reasons for cells to regulate ER export, including to regulate inter-cellular communication in the case of secretory cells and neurons, to limit infection by viruses, and to regulate resource consumption, cell size, growth and ER stress in all cells. We propose that under basal conditions, peflin and ALG-2 regulate the ER export rate through long-term adjustments involving changes in expression ratios of the two proteins and also shorter-term changes in the PEF species bound at ERES which may be responsive to spontaneous Ca^{2+} oscillations, the ER Ca^{2+} leak rate, and/or environmental Ca^{2+} conditions. However, we also identified an acute response to sustained agonist-driven Ca^{2+} signaling involving a drastic reduction in ER-to-Golgi transport within 1 hour, an apparent adaption of the secretory pathway to stressful conditions for which we have found no precedent in the literature. Execution of this response is entirely dependent on ALG-2, and full implementation of the response depends upon peflin as well. Though the short-term consequences of the secretion reduction may be protective to otherwise healthy cells, we speculated that it may be maladaptive to highly stressed cells.

Along these lines we focused on the single intervention that produces the largest change in secretion rate--knockdown of peflin--and applied this in a cellular model of ageing wherein primary porcine aorta endothelial cells become senescent, display mitochondrial Ca^{2+} excitotoxicity, elevated ROS production, chronic ER stress signaling in the absence of chemical

inducers, and eventual apoptosis (Madreiter-Sokolowski *et al.*, 2019). We found that peflin depletion drastically reduced pro-apoptotic UPR signaling, consistent with its suppressive role in secretion being highly relevant to damage-inducing ER stress.

While this work did not characterize the molecular states and mechanisms responsible for peflin and ALG-2 regulation of transport, previous work has characterized an ALG-2 homodimer interacting with a Sec31A peptide from the proline rich region (Takahashi *et al.*, 2015) which our studies would predict is the stimulatory interaction. Peflin and ALG-2 have also been demonstrated to reside in a 1:1 heterodimer in cytosol (Kitaura *et al.*, 2001), which our studies would predict binds to Sec31A through its ALG-2 subunit to inhibit transport. We note that in the homodimer configuration, ALG-2 subunits could crosslink distinct Sec31A molecules perhaps stimulating inner-outer coat interactions, which take place only a few residues downstream of the ALG-2 binding site on Sec31A. Previous studies with purified coat proteins and ALG-2 indeed found that ALG-2 was able to strongly potentiate binding between Sec31 and Sec23 without engaging in direct interactions with Sec23 itself (la Cour *et al.*, 2013). Perhaps the homodimer of ALG-2 crosslinks Sec31A molecules to activate a cooperative effect on its interactions with Sec23. The ALG-2/peflin heterodimer, on the other hand, would not be able to crosslink Sec31A molecules, and in the absence of the cooperativity might actually impede inner-outer coat interactions.

A previous study found that depletion of ALG-2 inhibits collagen transport in IMR-90 lung fibroblasts (Takahara *et al.*, 2017). Although we found that VSV-G transport in NRK cells increases, not decreases, when ALG-2 is depleted (Figure 1), our data does not necessarily conflict because our findings also demonstrate that the impact of ALG-2 depletion on secretion will depend upon peflin concentrations and signaling conditions in any given cell type--when the stimulatory ALG-2 species predominates, siALG-2 would inhibit transport in our cells too. On the other hand, our results and model are difficult to reconcile with a report suggesting that depletion of either peflin or ALG-2 inhibited collagen transport in human osteosarcoma cells (McGourty *et al.*, 2016). It is possible that peflin and ALG-2 have opposite roles in secretion in osteosarcoma cells and fibroblasts--both professional collagen-secreting cells. On the other hand, the earlier report did not measure ER-to-Golgi transport, but instead disappearance of collagen from the ER. Given that excess collagen is removed from the ER by other pathways, including non-canonical autophagy at ERES (Omari *et al.*, 2018), it is possible the discrepancy is

due to effects of PEF proteins on that pathway, which may be potentiated in osteosarcoma cells.

An unexpected discovery was that peflin is concentrated in the nucleus (Figure 2). The bright nuclear intensity was decreased significantly by peflin siRNA indicating that it represents specific antigen labeling. ALG-2 has also been reported to localize to, and is implicated in splicing reactions in the nucleus (Sasaki-Osugi *et al.*, 2013). While we cannot rule out the possibility that nuclear function of either ALG-2 or peflin could contribute to their transport effects, their presence and intensity ratios at ERES during expression studies (Figure 2) correlates extremely well with their functional impacts on ER-to-Golgi transport (Figure 1). We also note that knockdowns of peflin in unstressed cells under basal conditions did not detectably affect the unfolded protein response (UPR) as indicated by intensities of bands on Westerns with the following antibodies: anti-phospho-Ire1, anti-phosho-EIF2 alpha, and anti-ATF4 (data not shown). This excludes the mechanism wherein peflin depletion could cause ER stress which would increase transcription of COPII machinery to accelerate secretion. Based upon available evidence, we conclude that the PEF protein expression effects on ER-to-Golgi transport are mediated directly through interactions with Sec31A at ERES.

MATERIALS AND METHODS

Antibody Production and Purification

Rat peflin and mouse ALG-2 were ligated into pGEX expression plasmids and expressed in E.coli as GST fusion proteins. Cultures were grown at 37°C to an A_{600} of 0.4-0.6, prior to an induction with 1mM isopropyl-1-thio-β-D-galactopyranoside (IPTG) at 37°C for GST-ALG-2, and 15°C for GST-peflin, for 3 h. Harvested cells were subjected to a single round of French Press and centrifuged at 20, 000 x g for 20min. Pellets were collected, dissolved in sample buffer and loaded onto SDS–PAGE gels. Gels were stained with 0.1% Coomassie in H_20, and the resolved bands were excised from the gel and subjected to a 3 h electroelution in 25mM Tris, 191mM glycine and 0.1% SDS, on ice. The eluted protein solution was concentrated and injected subcutaneously, using Freund's adjuvant, into a rabbit, for peflin, or a chicken for ALG-2. Three subsequent antigen boost injections were done over an 80-day period. At this stage, the peflin antibody was fully useful as a crude serum. For the ALG-2 antibody, sera were supplemented with an equal volume of 10mM Tris, pH7.5, filtered with a syringe filter and passed through a

1ml CNBr-Sepharose column conjugated with GST as non-specific control. The flow through was then loaded onto another CNBr-Sepharose column conjugated with mouse GST-ALG-2. Columns were washed with 3 x 5ml of 10mM Tris, pH 7.5, then washed with the same buffer containing 0.5M NaCl, once again with 10mM Tris, pH 7.5 and finally eluted with 0.1M glycine, pH 2.5. Fractions were neutralized with 2 M Tris, pH 8.0, and quantitated at A280. Peak fractions were pooled and dialyzed into PBS.

Other antibodies and expression constructs

Anti-VSVG was purchased from Sigma-Aldrich St. Louis, MO (product: V5507, clone P5D4). Mouse monoclonal anti-CHOP antibody was purchased from ThermoFisher Scientific, Waltham, MA (product: MA1-250). Rabbit polyclonal anti-collagen I antibody was purchased from Abcam, Cambridge, UK (product: ab34710). Mouse monoclonal anti-mannosidase II antibody was purchased from Covance Research Products, Denver, PA (product: MMS-110R-200). Green secondary antibodies were from Invitrogen (Carlsbad, CA), Alexa Flour^{TM} 488 (product: A11001); Cy3-, or cy5-conjugated secondary antibodies were purchased from Jackson ImmunoResearch Laboratories (West Grove, PA). Constructs designated by,'*' are used as a synchronizeable cargo for ER-to-Golgi transport studies. Human GFP-Collagen I* was from David Stephens via Addgene, Cambridge, MA (construct: pEGFp-N2-COL1A1). For overexpression studies peflin and ALG-2 constructs were utilized. Rat peflin was amplified from a cDNA clone by PCR primers encoding EcoR1/XhoI. This product was ligated into mammalian expression vector PCDNA 3.1(+). Mouse ALG-2 was cloned from a cDNA clone (MGC: 49479) and ligated into mammalian expression vector pME18S by PCR primers XhoI/XbaI. GFP-Sec13 was as described (Hammond and Glick, 2000) . For total cell fluorescence calculations pCAG-mGFP was purchased from Addgene (product: 14757). The transport cargos retained in the ER until triggered to export with a ligand are based upon the RPD Regulated Secretion/Aggregation Kit from ARIAD Pharmaceuticals. The luminal cargo we here call "GFP-F_M4-GH"* is in fact identical to the construct pC4S1-eGFP-FM4-FCS-hGH we described before (Gordon *et al.*, 2010). GFP-F_M4-VSVG_{tm}* was constructed by removing the furin cleavage site and human growth hormone by cleavage with SpeI/BamHI and replacing it with a fragment containing the VSVG transmembrane domain: 5'-actagtTCATCGTCGAAGAGCTCTATTGCCTCTTTTTTCTTTATCATAGGGTTAATCATTG

GACTATTCTTGGTTCTCCGAGTTGGTATTTATCTTTGCATTAAATTAAAGCACACCAA GAAAAGACAGATTTATACAGACATAGAGATGAACCGACTTGGAAAGTAAGCGCCCG Cggatcc-3' To make GFP-F_M4-GPI* was the same procedure except that the SpeI/BamHI-cleaved construct was ligated with a fragment containing the CD55 GPI anchor sequence: 5-actagtACAACCCCAAATAAAGGAAGTGGAACCACTTCAGGTACTACCCGTCTTCTATC TGGGCACACGTGTTTCACGTTGACAGGTTTGCTTGGGACGCTAGTAACCATGGGCTT GCTGACTTAGggatcc-3' This construct is targeted to the plasma membrane where it is sensitive to extracellular PI-PLC treatment.

siRNA knockdowns and transfections

For transport experiments NRK cells were electroporated with 0.6 µM siRNA (Custom siRNAs synthesized from GeneLink™, Orlando, FL) and grown in high glucose DMEM containing 10% fetal calf serum and penicillin-streptomycin. After 2-3 days of normal growth at 37 °C, the cells were resuspended and re-electroporated, this time with a combination of the siRNA plus 7.5 µg of cargo DNA expression plasmid. Cells were allowed to recover and grow on coverslips at 41 °C for 24 h. Cells from all transfections were either lysed directly in Sample buffer for quantitative immunoblotting, or else processed for transport or colocalization assays as described below. Control siRNA had the following sense strand sequence: 5' - AGGUAGUGUAAUCGCCUUGdTdT- 3'. Peflin and ALG-2 siRNAs were described previously (Helm *et al.*, 2014; Rayl *et al.*, 2016). Collagen siRNA had the following sense strand sequence: 5'-GAACUCAACCUAAAUUAAAdTdT-3'. Immunoblotting of cell lysates enabled validation of knockdown efficiencies for each siRNA experiment that was functionally analyzed. We have confirmed previously, that the effects on secretion of peflin and ALG-2 siRNAs are common to at least three non-overlapping, distinct siRNAs (Helm *et al.*, 2014; Rayl *et al.*, 2016).

Cell Culture and Histamine Treatments

Normal rat kidney (NRK) and rat 2 fibroblasts (R2) were purchased from ATCC. Both lines were treated the same and were grown at 37 °C using high glucose DMEM supplemented with 10% fetal calf serum, and 1% penicillin-streptomycin. Porcine aorta endothelial cells were isolated and cultured to P5 as described before (Madreiter-Sokolowski *et al.*, 2019). For

histamine treatments transfected and/or siRNA-transfected NRK cells were grown to 25-75% confluency in 6-well chambers. 1ml solutions of histamine (Sigma H7125) were prepared fresh each day at a concentration of 100mM. 41 ^{o}C NRK cells growing in culture media were supplemented with histamine at a concentration of 100µM for 0 min to 2.5 h.

Calcium Imaging

Subconfluent NRK cells growing on glass coverslips were transfected with the cytosolic Ca^{2+} sensor D3cpv (Palmer *et al.*, 2006) using Polyjet transfection reagent (SignaGen Laboratories, Rockville MD, USA). The next day, coverslips were placed in a perfusion chamber and perfused with $2Ca^{2+}$ buffer (2 mM $CaCl_2$, 138 mM NaCl, 1 mM $MgCl_2$, 5 mM KCl, 10 mM D-glucose, 10 mM Hepes, pH 7.4) at 2 ml/min at room temperature on a Nikon TE300 inverted microscope equipped with a 60x objective, motorized high speed Sutter Lambda filter wheel for emissions, CoolLED pe340 excitation system, and PCO Panda sCMOS camera, all automated with Micro-Manager software. After selecting a field with transfected cells, imaging was carried out for 30 minutes with 5-second intervals; for each interval, an image was collected at 480 nm and 530 nm using 430 nm excitation. After 6.5 min, the running buffer was changed to $2Ca^{2+}$ + 100 µM histamine, and then back to $2Ca^{2+}$ again at 26.5 min. For analysis in Fiji, each cell, as well as an extracellular background region was enclosed in an ROI and mean intensity was collected in each color channel at each time interval. Data was imported to Kaleidagraph software, where the intensity data was converted to FRET ratios represented by (emission at 530 -background at 530)/(emission at 480 -background at 480). The FRET ratio curves were then fit to an exponential decay function to remove effects of progressive photo-bleaching during the recording, and finally converted to R/R_0 by dividing every R value by the initial R value for each trace.

PAEC's and RT-PCR

Aged PAECs were transfected with peflin siRNA using Transfast (Promega Corp., Madison WI, USA) using manufacturer's instructions. Total RNA was isolated using the PEQLAB total RNA isolation kit (Peqlab; Erlangen, Germany) and reverse transcription was performed in a thermal cycler (Peqlab) using a cDNA synthesis kit (Applied Biosystems; Foster City, CA). mRNA levels were examined by qRT-PCR. A QuantiFast SYBR Green RT-PCR kit (Qiagen; Hilden,

Germany) was used to perform real time PCR on a LightCycler 480 (Roche Diagnostics; Vienna, Austria), and data were analyzed by the REST Software (Qiagen). Relative expression of specific genes was normalized to human GAPDH as a housekeeping gene. Primers for real time PCR were obtained from Invitrogen (Vienna, Austria).

Immunofluorescence microscopy

Coverslips were fixed with 4% paraformaldehyde containing 0.1M sodium phosphate (pH 7) for 30 min at room temperature and quenched three times for 10 min with PBS containing 0.1M glycine. Fixed cells were treated for 15 min at room temperature with permeabilization solution containing 0.4% saponin, 1% BSA, and 2% normal goat serum dissolved in PBS. The cells were then incubated with primary antibodies diluted in permeabilization solution for 1 h at room temperature. Next, coverslips were washed 3x with permeabilization solution and incubated 30 min at room temperature with different combinations of Alexa Flour^{TM} 488-, Cy3-, and/or Cy5-conjugated anti-mouse, anti-rabbit, or anti-chicken secondary antibodies. After the secondary antibody incubation, coverslips were again washed 3x using permeabilization solution and mounted on glass slides using Slow Fade Gold antifade reagent (Invitrogen: S36936) and the edges sealed with nail polish. Slides were analyzed using a 40x or 60x objective on a Nikon E800 microscope with an LED illumination unit (CoolLED pE 300^{white}), sCMOS PCO.edge 4.2 camera, Prior excitation and emission filter wheels and Z-drive, automated using Micro-Manager software. For transport assays (see below) typical images collected for each field of cells were VSV-G-GFP (GFP channel), and Golgi marker Mannosidase II (cy5 channel). For colocalization assays (see below) typical images collected for each field of cells were Sec13-EGFP (GFP channel), ALG-2 (cy3 channel), and Peflin (cy5 channel).

ER-to-Golgi transport assay

NRK cells were transfected and knocked down as described above and plated on Poly-L-lysine coated coverslips. After 24 hours of cargo plasmid expression at 41 ^{o}C, the cells were either fixed by dropping coverslips directly into fixative or into 6-well chambers containing pre-equilibrated 32 ^{o}C medium for 10 min, then transferred to fixative. For assays involving Collagen I cargo the 32 ^{o}C medium was supplemented with 50µg/ml ascorbate. Coverslips were fixed and labeled as described above. Alternately, after 24 h of F_m4-cargo expression in NRK

cells kept at 37 ^{o}C, cell coverslips were either fixed by dropping coverslips directly into fixative or dropped into to 6-well chambers containing 37 ^{o}C media with 500nM AP21998, also known as D/D solubilizer (TakaraBio, Shiga Japan: 635054), for 10 min prior to transfer to fixative.

Morphological quantitation of ER-to-Golgi transport was accomplished by first collecting images in a consistent manner with regard to cell morphology, protein expression levels and exposure. We selected a fixed exposure time for each color channel that would accommodate the vast majority of cells. A single widefield image plane was collected for each color channel for each field of cells randomly encountered; image deconvolution was not performed. Prior to image analysis using a custom script (available upon request), files for all experimental conditions were randomly renamed with a 36- character designation, and re-sorted by that identifier. Old image titles, and the name they were changed to were stored as a key in a csv file; the key was not opened until all quantitation was complete. This eliminated any bias the quantitator may have during the process. Images were analyzed using Fiji open source image software with automation by a custom script. On the GFP image plane, the user defines the minimal rectangular ROI encompassing the cell to be analyzed, making certain that some dark, extracellular regions are represented along at least one edge of the ROI. This ROI is then isolated in a separate window and two parameters extracted; background, which represents the highest pixel intensity among the lowest 0.100 percentile of nonzero pixel values; and Golgi maximum, which represents the mean intensity of the pixels in the 99.990 percentile and above but excluding the highest pixel. The user checks that these brightest pixels are in fact within the Golgi as defined on the mannosidase II image planes. The user then sequentially defines 3 small square ROIs within vesicular/reticular regions adjacent to the nucleus but clearly distinct from the Golgi area and avoiding thin areas of cytoplasm near the edge of the cell. The ER mean was extracted as the mean of the three mean pixel intensities of these ROIs. Transport index was then calculated for each individual cell as (Golgi maximum-background) / (ER mean-background). The cell was then numbered on the image to avoid re-counting, and all extracted parameters written to an appendable output file along with the cell number, and image title so that the data was traceable. The user then defines another cell from the image or opens another image. Using this method, the user quantitates about 60 cells per hour.

Once transport indices have been obtained for all conditions in an experiment, each value is subtracted by the mean transport index value for cells that were fixed directly from 40 ^{o}C without

a transport incubation at 32 ^{o}C (typically a value between 1.0 and 1.5) to generate the net transport index. This transport index was then reassigned from its associated randomized filename to its original filename, and the data are re-sorted by experimental conditions. Net transport indices are then normalized to the mean siControl value for the particular experiment, prior to plotting and comparison between experiments. Each result reported here was obtained in at least three separate experiments on different days.

Colocalization Assays

For immunofluorescence co-localization experiments NRK cells were grown in DMEM high glucose containing 10% fetal calf serum and penicillin-streptomycin. Fixed cells such as in Figure 2 were captured as z-stacks in eleven 200 nm increments for each color channel. These image stacks were deconvolved using Huygens Essential Widefield software (Scientific Volume Imaging, Hilversum, The Netherlands). Final images for display and quantitation represent maximum intensity projections of deconvolved stacks. As before these deconvolved stacks were assigned a random 36-character designation, with the old and new filename stored in a csv file. ERES intensity was assessed by a custom FIJI script (available upon request). Background labeling was removed by defining a dark extracellular area of each channel image as zero. Next a GFP-Sec13 object binary image mask was generated by auto thresholding using the Renyi Entropy method, all spots were assessed as a single ROI, and that same ROI was used to measure integrated density (product of area and mean intensity) in the ALG-2 and peflin channels. All extracted parameters were written to an appendable output file along with the cell number and image title so that the data was traceable. Following re-sorting by experimental conditions, integrated densities for each cell were then normalized to the mean siControl value for the particular experiment, prior to plotting and comparison as reported in figure 2. Each result reported here was obtained in at least three separate experiments, though the data shown in Figure 2 are from a single replicate.

Total Cell Fluorescence Assay

As in Figures 4B-C, total cell fluorescence of collagen was determined by first transfecting R2 cells with the plasma membrane marker pCAG-mGFP (GFP with an N-terminal palmitoylation signal). Endogenous collagen I was labelled in the cy3 channel. Using pCAG-mGFP a whole cell

ROI was selected via the wand threshold tool in FIJI. That ROI was then moved into the collagen channel wherein total mean gray values and ROI area were extracted. Separately, a mean background value was extracted by randomly selecting an area without a cell. Total cell fluorescence was calculated using the formula, Integrated Density – (Area of selected cell x Mean fluorescence of background reading).

ACKNOWLEDGMENTS

This work was supported by NIH grant 1R15GM106323-02 to JCH. The authors also thank University of Montana undergraduate students Danette Seiler, Emily Peinado and Samuel Wrobel for technical assistance with experiments.

FIGURE LEGENDS

Figure 1. Dynamic range of secretion controlled by PEF proteins. (A) NRK cells were transfected with VSV-G_{ts045}-GFP with or without siRNAs and untagged over-expression constructs for peflin or ALG-2. Following growth at 41 ^{o}C for 24 hours, cells were shifted to 32 ^{o}C for 10 minutes, to permit transport, prior to fixation. Fixed cells were labeled with mannosidase II. Each transfected cell was assigned a transport index representing trafficking of VSV-G based upon the ratio of Golgi to peripheral green fluorescence. The transport index of each individual cell is plotted. Approximately 200 cells were randomly quantified from each condition, and results shown are representative of at least 3 experiments with consistent trends. *p*-values for two-tailed Student T-tests with unequal variance are indicated above. Standard error is shown for each plot. **(B)** Example widefield images of individual cells for select conditions with their transport index indicated.

Figure 2. Peflin-ALG2 hetero-oligomers localize to ER exit sites via ALG-2, competing other ALG-2 species. NRK cells were transfected with GFP-sec13 with or without siRNAs and an untagged rat over-expression construct for peflin. **(A)** Intensity values of peflin at ERES marked by GFP-sec13, wherein each point represents a single cell. Transfection conditions are specified below the graph and *p* values for select comparisons are indicated. Standard error is shown for each condition. **(B)** Intensity values of ALG-2 at ERES marked by GFP-sec13. **(C)** Immunofluorescence images of endogenous NRK cell peflin and ALG-2. ERES marked by

GFP-sec13. Magenta circles highlight ERES containing peflin or ALG2 that co-localizes with GFP-Sec13, while green circles note the absence of co-localization with GFP-Sec13. Transfection conditions are specified to the left of images.

Figure 3. Peflin expression suppresses ER export of multiple actively exported cargos in NRK cells. (A) The initial rate of ER-to-Golgi transport was determined as in Figure 1 for NRK cells transfected with the indicated constructs in the presence or absence of peflin siRNA. For VSV-G_{ts045}-GFP and GFP-collagen I, transfected cells were placed at 41 ^{o}C for 48 hours to build up cargo in the ER, and transfer of cells to 32 ^{o}C provided a synchronous wave of transport to the Golgi. For GFP-F_M4-VSVG_{tm}, GFP-F_M4-GPI, and GFP-F_M4-GH, cargo was accumulated in the ER under normal growth conditions at 37 ^{o}C, and was released for transport by addition of the F_M4-specific ligand. Unpaired T-test *p* values are displayed for the indicated comparisons. Mean ± SEM is shown for each condition. **(B)** Example widefield images of individual cells for select conditions. For GFP-collagen I, a merge of GFP and the Golgi marker Mannosidase II is shown; all other images are GFP-only.

Figure 4. Peflin expression suppresses ER export of endogenous collagen I in Rat2 fibroblasts. Rat2 cells were transfected with the plasma membrane marker pCAG-mGFP and grown in the presence or absence of peflin siRNA. Following growth at 41 ^{o}C for 24 hours, cells were shifted to 32 ^{o}C, with 50μg/ml ascorbate, for 15 minutes, to permit transport, prior to fixation. **(A)** Temperature-shifted R2 cells underwent an ER-to-Golgi transport assay and a transport index for each cell was calculated, and plotted; n = ~200. **(B)** The same cells used in "A" were assigned a value for total cell fluorescence of collagen. Total collagen I content was not significantly affected while ER-to-Golgi transport was significantly enhanced in the absence of peflin in the same cells. **(C)** Validation of immunofluorescence assay for total cell fluorescence of collagen I. Cells were transfected with different concentrations of collagen I siRNA or an siRNA for peflin, demonstrating no significant effect of peflin knockdown on the total cell content of collagen I. Standard error is shown for each plot. **(D)** Example widefield images of collagen I staining for select conditions in individual cells.

Figure 5. Ca^{2+} signaling-dependent suppression of ER export is mediated by PEF

proteins. (A) NRK cells were transfected with the FRET-based Ca^{2+} sensor D3cpv. NRK cells were perfused with an extracellular buffer for 6.5 min before addition of 100 μM histamine (black bar) for 20 min and then removed. FRET traces show data from two representative cells. **(B)** NRK cells were transfected with VSV-G_{ts045}-GFP along with control, ALG-2, or peflin siRNAs. Transfected cells were exposed to 100 μM histamine for 0 min to 2.5 hr at the non-permissive temperature prior to shift to the permissive temperature for 10 min, and transport was quantitated as in Figure 1. Mean ± SEM is shown for each point; n~150 cells per condition. **(C)** Example widefield images of individual cells for select conditions. **(D)** The rate of ER-to-Golgi transport following peflin overexpression and/or histamine exposure was determined as in Figure 1.

Figure 6. Peflin expression facilitates pro-apoptotic UPR signaling. Peflin depletion in P5 PAECs dramatically reduces GRP78 and CHOP expression. Senescent P5 PAECs were subjected to control or siPeflin siRNA transfection and grown under standard conditions for 3 days prior to lysis and analysis by qRT-PCR for expression of several mRNAs as indicated beneath the plot. Results are shown as the ratio of mRNA expression in siPEF cells to that in siControl cells for each mRNA. Bars show mean ± SEM for 3 complete experiments conducted on different days. Asterisks indicate p values for unpaired T test for each condition vs. the null hypothesis value of 1.0. **, $p<.005$; ***, $p<.0005$

REFERENCES

Bentley, M., Nycz, D. C., Joglekar, A., Fertschai, I., Malli, R., Graier, W. F., and Hay, J. C. (2010). Vesicular calcium regulates coat retention, fusogenicity, and size of pre-Golgi intermediates. Mol Biol Cell *21*, 1033–1046.

Bi, X., Mancias, J. D., and Goldberg, J. (2007). Insights into COPII coat nucleation from the structure of Sec23.Sar1 complexed with the active fragment of Sec31. Dev. Cell *13*, 635–645.

Bonnon, C., Wendeler, M. W., Paccaud, J.-P., and Hauri, H.-P. (2010). Selective export of human GPI-anchored proteins from the endoplasmic reticulum. J Cell Sci *123*, 1705–1715.

Ghaemmaghami, S., Huh, W.-K., Bower, K., Howson, R. W., Belle, A., Dephoure, N., O'Shea, E. K., and Weissman, J. S. (2003). Global analysis of protein expression in yeast. Nature *425*, 737–741.

Gordon, D. E., Bond, L. M., Sahlender, D. A., and Peden, A. A. (2010). A targeted siRNA screen to identify SNAREs required for constitutive secretion in mammalian cells. Traffic *11*, 1191–1204.

Hammond, A. T., and Glick, B. S. (2000). Dynamics of transitional endoplasmic reticulum sites in vertebrate cells. Mol Biol Cell *11*, 3013–3030.

Helm, J. R., Bentley, M., Thorsen, K. D., Wang, T., Foltz, L., Oorschot, V., Klumperman, J., and Hay, J. C. (2014). Apoptosis-linked gene-2 (ALG-2)/Sec31 interactions regulate endoplasmic reticulum (ER)-to-Golgi transport: a potential effector pathway for luminal calcium. J Biol Chem *289*, 23609–23628.

Hughes, H., and Stephens, D. J. (2008). Assembly, organization, and function of the COPII coat. Histochem Cell Biol *129*, 129–151.

Kitaura, Y., Matsumoto, S., Satoh, H., Hitomi, K., and Maki, M. (2001). Peflin and ALG-2, members of the penta-EF-hand protein family, form a heterodimer that dissociates in a Ca2+-dependent manner. J Biol Chem *276*, 14053–14058.

Kitaura, Y., Satoh, H., Takahashi, H., Shibata, H., and Maki, M. (2002). Both ALG-2 and peflin, penta-EF-hand (PEF) proteins, are stabilized by dimerization through their fifth EF-hand regions. Arch Biochem Biophys *399*, 12–18.

la Cour, J. M., Mollerup, J., and Berchtold, M. W. (2007). ALG-2 oscillates in subcellular localization, unitemporally with calcium oscillations. Biochem Biophys Res Commun *353*, 1063–1067.

la Cour, J. M., Schindler, A. J., Berchtold, M. W., and Schekman, R. (2013). ALG-2 attenuates COPII budding in vitro and stabilizes the Sec23/Sec31A complex. PLoS ONE *8*, e75309.

Ma, W., Goldberg, E., and Goldberg, J. (2017). ER retention is imposed by COPII protein

sorting and attenuated by 4-phenylbutyrate. Elife *6*, 213.

Madreiter-Sokolowski, C. T. *et al.* (2019). Enhanced inter-compartmental Ca2+ flux modulates mitochondrial metabolism and apoptotic threshold during aging. Redox Biol *20*, 458–466.

Maki, M., Kitaura, Y., Satoh, H., Ohkouchi, S., and Shibata, H. (2002). Structures, functions and molecular evolution of the penta-EF-hand Ca2+-binding proteins. Biochim Biophys Acta *1600*, 51–60.

McCaughey, J., Miller, V. J., Stevenson, N. L., Brown, A. K., Budnik, A., Heesom, K. J., Alibhai, D., and Stephens, D. J. (2016). TFG Promotes Organization of Transitional ER and Efficient Collagen Secretion. Cell Rep *15*, 1648–1659.

McGourty, C. A., Akopian, D., Walsh, C., Gorur, A., Werner, A., Schekman, R., Bautista, D., and Rape, M. (2016). Regulation of the CUL3 Ubiquitin Ligase by a Calcium-Dependent Co-adaptor. Cell *167*, 525–538.e14.

Miller, E. A., and Barlowe, C. (2010). Regulation of coat assembly--sorting things out at the ER. Curr Opin Cell Biol *22*, 447–453.

Omari, S., Makareeva, E., Roberts-Pilgrim, A., Mirigian, L., Jarnik, M., Ott, C., Lippincott-Schwartz, J., and Leikin, S. (2018). Noncanonical autophagy at ER exit sites regulates procollagen turnover. Proc Natl Acad Sci USA *115*, E10099–E10108.

Palmer, A. E., Giacomello, M., Kortemme, T., Hires, S. A., Lev-Ram, V., Baker, D., and Tsien, R. Y. (2006). Ca2+ indicators based on computationally redesigned calmodulin-peptide pairs. Chem. Biol. *13*, 521–530.

Raote, I., Ortega-Bellido, M., Santos, A. J., Foresti, O., Zhang, C., Garcia-Parajo, M. F., Campelo, F., and Malhotra, V. (2018). TANGO1 builds a machine for collagen export by recruiting and spatially organizing COPII, tethers and membranes. Elife *7*, 2639.

Rayl, M., Truitt, M., Held, A., Sargeant, J., Thorsen, K., and Hay, J. C. (2016). Penta-EF-Hand Protein Peflin Is a Negative Regulator of ER-To-Golgi Transport. PLoS ONE *11*, e0157227.

Rivera, V. M. *et al.* (2000). Regulation of protein secretion through controlled aggregation in the endoplasmic reticulum. Science *287*, 826–830.

Saito, K., Chen, M., Bard, F., Chen, S., Zhou, H., Woodley, D., Polischuk, R., Schekman, R., and Malhotra, V. (2009). TANGO1 facilitates cargo loading at endoplasmic reticulum exit sites. Cell *136*, 891–902.

Sasaki-Osugi, K., Imoto, C., Takahara, T., Shibata, H., and Maki, M. (2013). Nuclear ALG-2 protein interacts with Ca2+ homeostasis endoplasmic reticulum protein (CHERP) Ca2+-dependently and participates in regulation of alternative splicing of inositol trisphosphate receptor type 1 (IP3R1) pre-mRNA. J Biol Chem *288*, 33361–33375.

Shibata, H., Inuzuka, T., Yoshida, H., Sugiura, H., Wada, I., and Maki, M. (2010). The ALG-2

binding site in Sec31A influences the retention kinetics of Sec31A at the endoplasmic reticulum exit sites as revealed by live-cell time-lapse imaging. Biosci. Biotechnol. Biochem. *74*, 1819–1826.

Shibata, H., Kanadome, T., Sugiura, H., Yokoyama, T., Yamamuro, M., Moss, S. E., and Maki, M. (2015). A new role for annexin A11 in the early secretory pathway via stabilizing Sec31A protein at the endoplasmic reticulum exit sites (ERES). J Biol Chem *290*, 4981–4993.

Shibata, H., Suzuki, H., Yoshida, H., and Maki, M. (2007). ALG-2 directly binds Sec31A and localizes at endoplasmic reticulum exit sites in a Ca2+-dependent manner. Biochem Biophys Res Commun *353*, 756–763.

Stagg, S. M., LaPointe, P., Razvi, A., Gürkan, C., Potter, C. S., Carragher, B., and Balch, W. E. (2008). Structural basis for cargo regulation of COPII coat assembly. *134*, 474–484.

Tabata, K., Sato, K., Ide, T., Nishizaka, T., Nakano, A., and Noji, H. (2009). Visualization of cargo concentration by COPII minimal machinery in a planar lipid membrane. Embo J.

Takahara, T., Inoue, K., Arai, Y., Kuwata, K., Shibata, H., and Maki, M. (2017). The calcium-binding protein ALG-2 regulates protein secretion and trafficking via interactions with MISSL and MAP1B. J Biol Chem, jbc.M117.800201.

Takahashi, T. *et al.* (2015). Structural analysis of the complex between penta-EF-hand ALG-2 protein and Sec31A peptide reveals a novel target recognition mechanism of ALG-2. Int J Mol Sci *16*, 3677–3699.

Wilson, D. G. *et al.* (2011). Global defects in collagen secretion in a Mia3/TANGO1 knockout mouse. J. Cell Biol. *193*, 935–951.

Yamasaki, A., Tani, K., Yamamoto, A., Kitamura, N., and Komada, M. (2006). The Ca2+-binding protein ALG-2 is recruited to endoplasmic reticulum exit sites by Sec31A and stabilizes the localization of Sec31A. Mol Biol Cell *17*, 4876–4887.

Yoshibori, M., Yorimitsu, T., and Sato, K. (2012). Involvement of the penta-EF-hand protein Pef1p in the Ca2+-dependent regulation of COPII subunit assembly in Saccharomyces cerevisiae. PLoS ONE *7*, e40765.

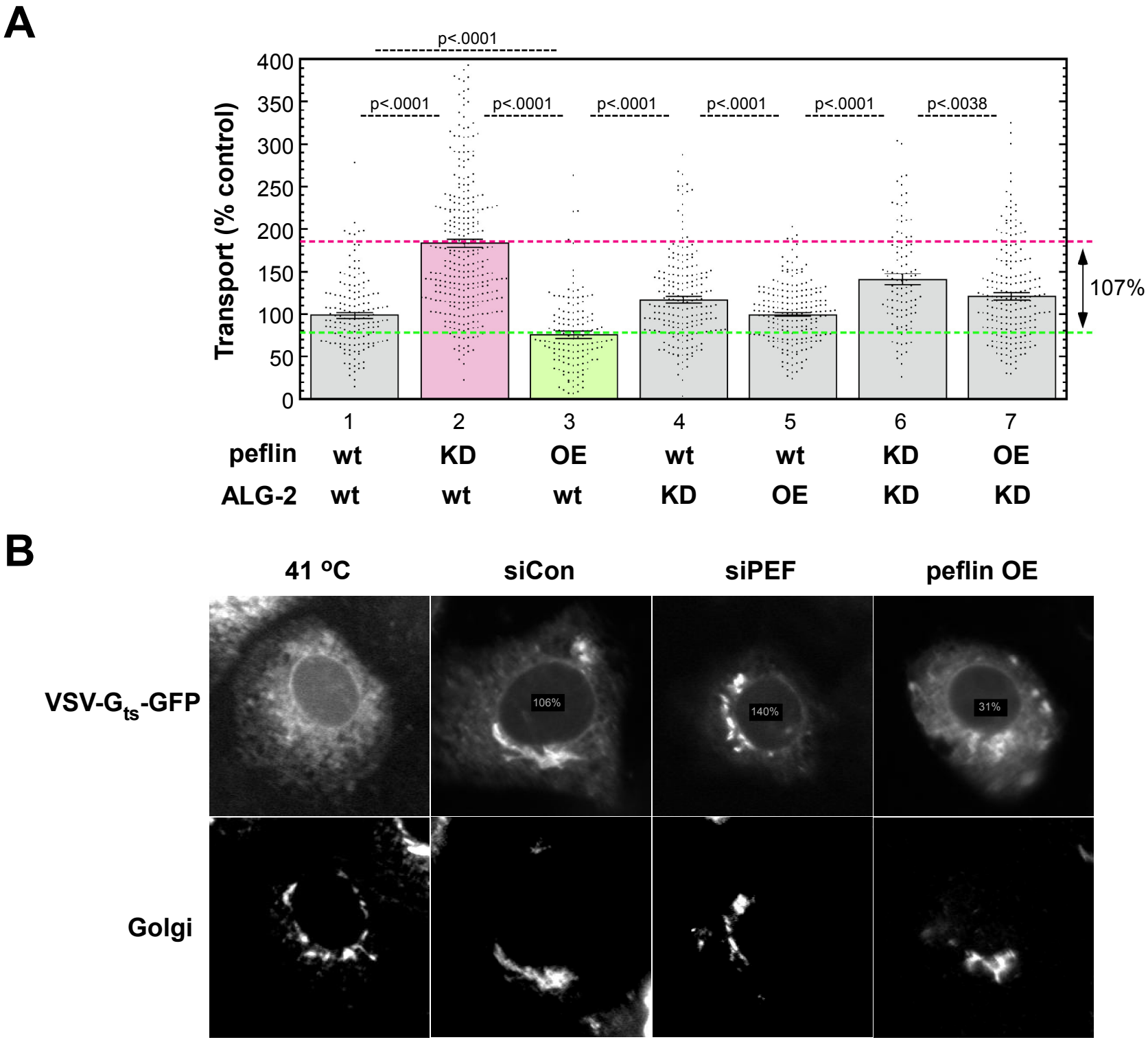
A
p<.0001
p<.0001
p<.0001
p<.0001
p<.0001
p<.0001
p<.0038
Transport (% control)
400
350
300
250
200
150
100
50
0
107%
1
2
3
4
5
6
7
peflin wt KD OE wt wt KD OE
ALG-2 wt wt wt KD OE KD KD
B
41 ºC
siCon
siPEF
peflin OE
VSV-G$_{ts}$-GFP
Golgi
106%
140%
31%

Fig 1

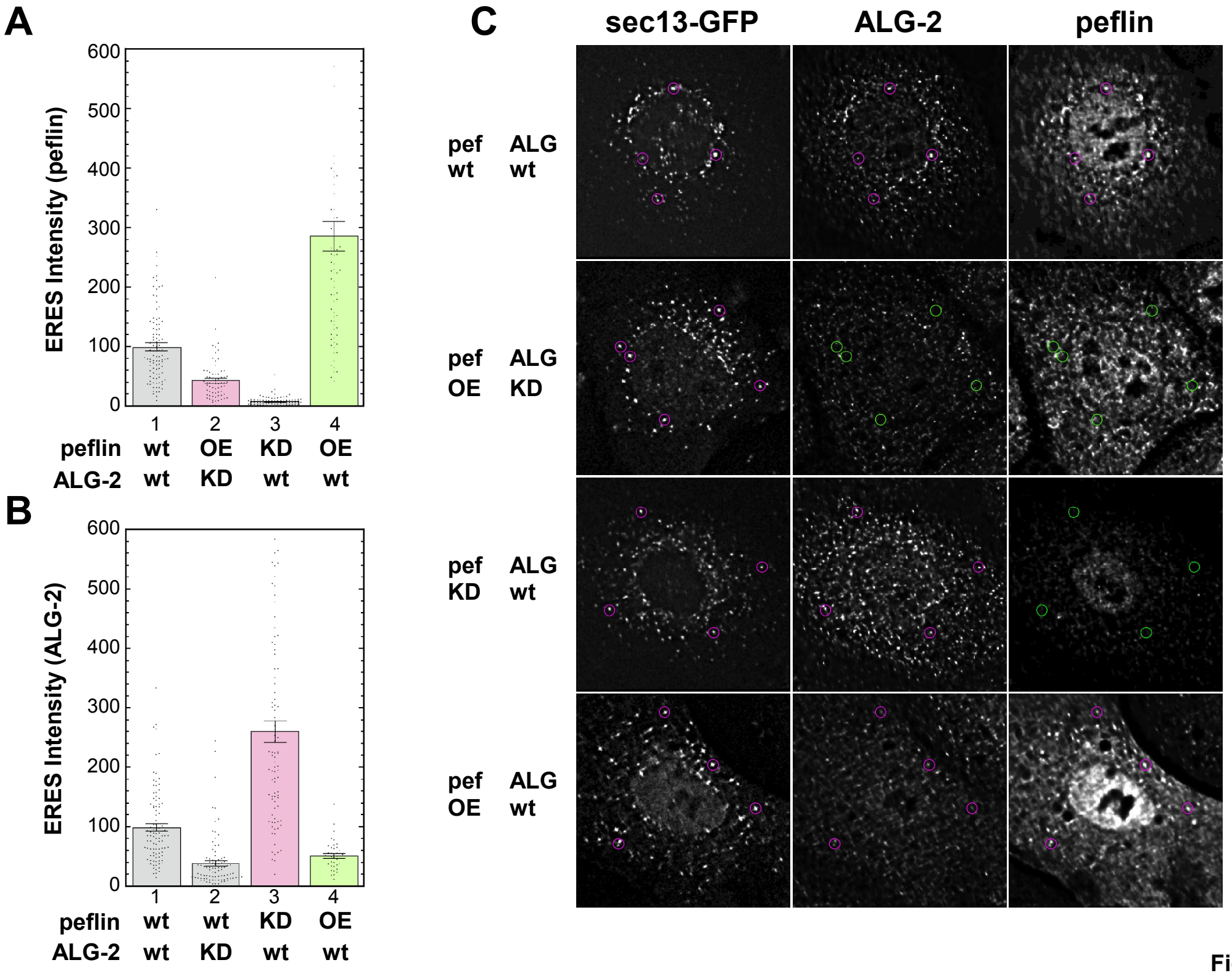
A
ERES Intensity (peflin)
600
500
400
300
200
100
0
1
2
3
4
peflin wt OE KD OE
ALG-2 wt KD wt wt
B
ERES Intensity (ALG-2)
600
500
400
300
200
100
0
1
2
3
4
peflin wt wt KD OE
ALG-2 wt KD wt wt
C
sec13-GFP
ALG-2
peflin
pef wt ALG wt
pef OE ALG KD
pef KD ALG wt
pef OE ALG wt

Fig 2

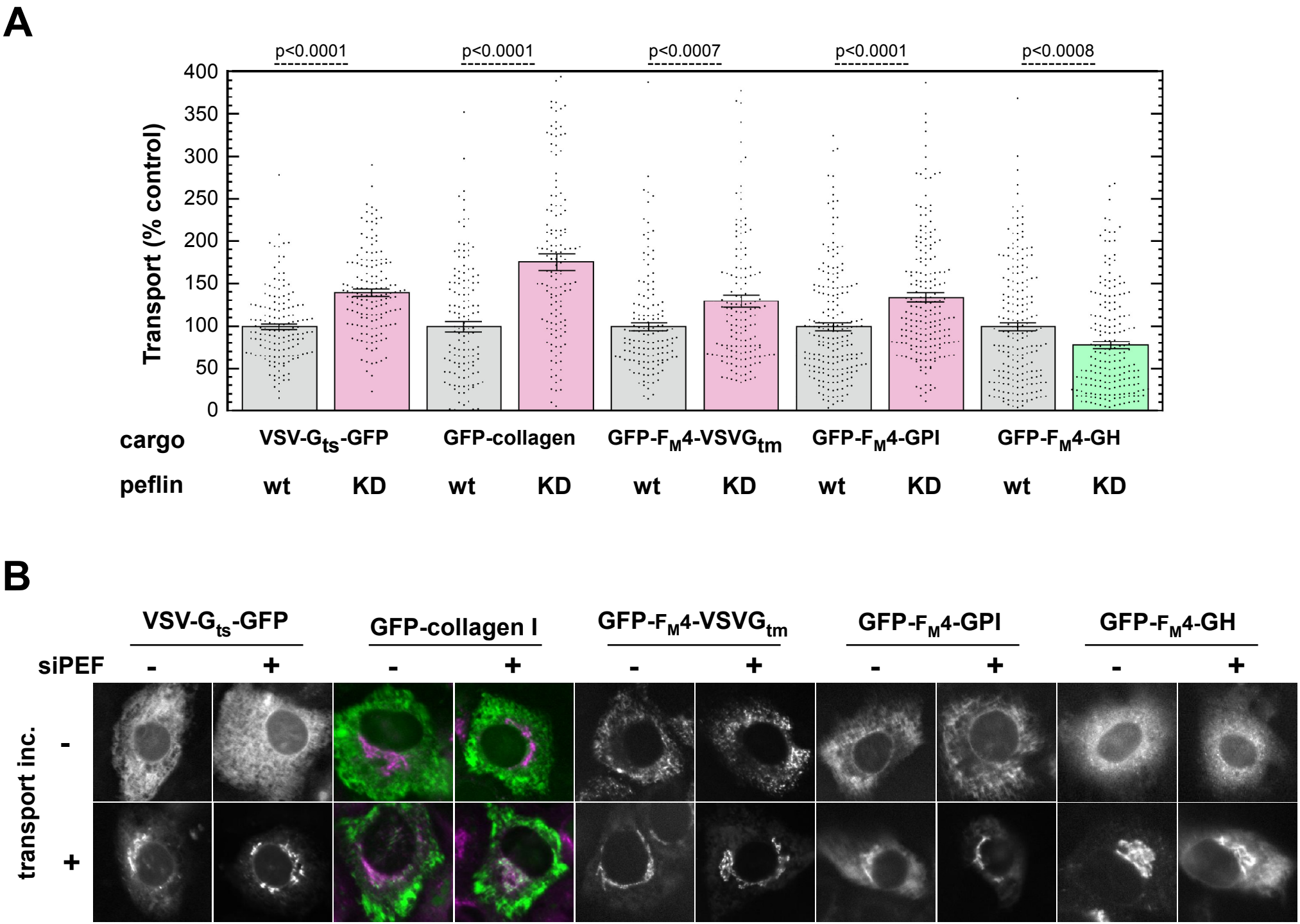
A
p<0.0001
p<0.0001
p<0.0007
p<0.0001
p<0.0008
Transport (% control)
400
350
300
250
200
150
100
50
0
cargo
VSV-Gts-GFP
GFP-collagen
GFP-FM4-VSVGtm
GFP-FM4-GPI
GFP-FM4-GH
peflin
wt
KD
wt
KD
wt
KD
wt
KD
wt
KD
B
VSV-Gts-GFP
GFP-collagen I
GFP-FM4-VSVGtm
GFP-FM4-GPI
GFP-FM4-GH
siPEF
-
+
-
+
-
+
-
+
-
+
transport inc.
-
+

Fig 3

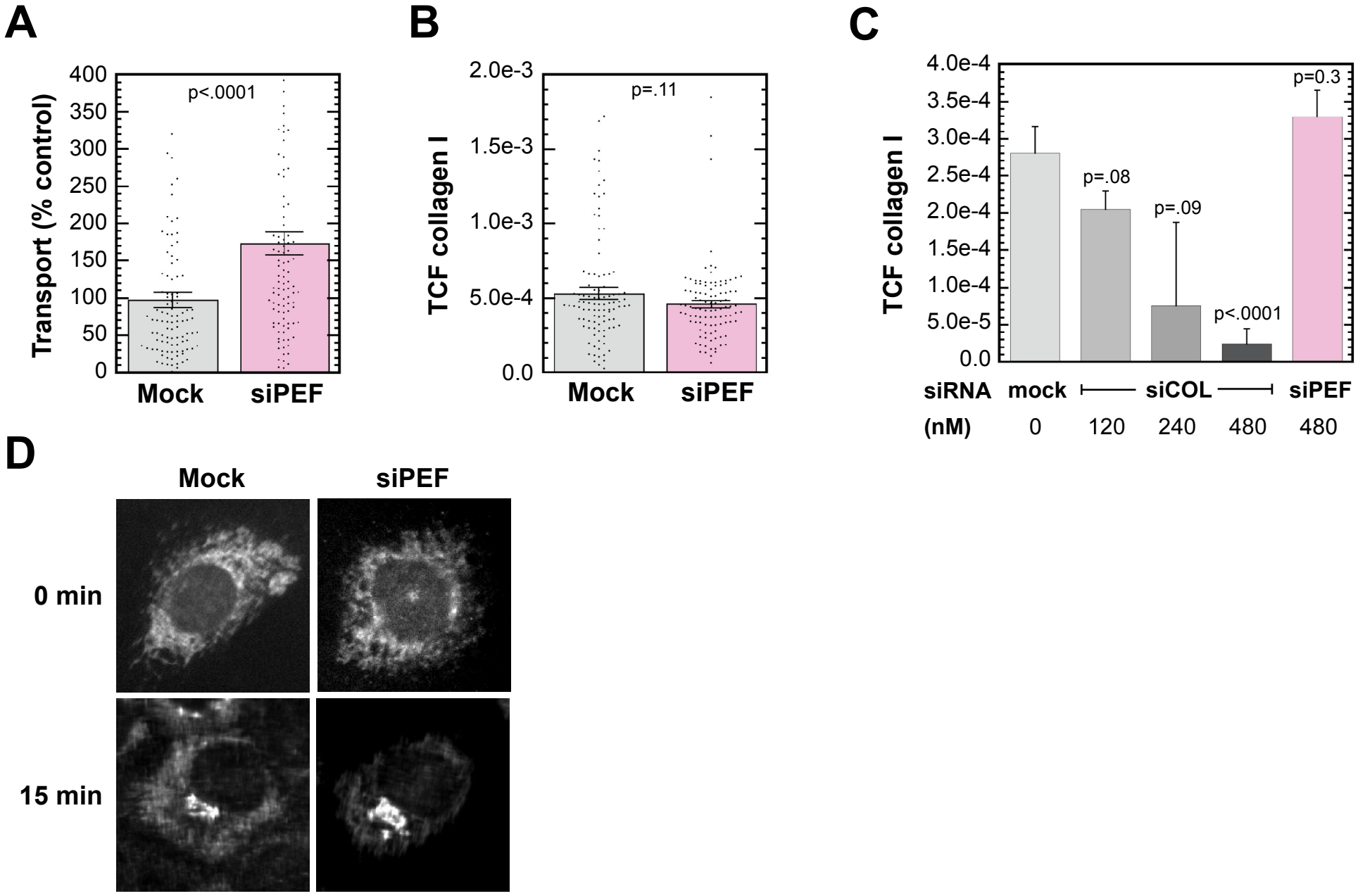
A
Transport (% control)
400
350
300
250
200
150
100
50
0
p<.0001
Mock
siPEF
B
TCF collagen I
2.0e-3
1.5e-3
1.0e-3
5.0e-4
0.0
p=.11
Mock
siPEF
C
TCF collagen I
4.0e-4
3.5e-4
3.0e-4
2.5e-4
2.0e-4
1.5e-4
1.0e-4
5.0e-5
0.0
p=.08
p=.09
p<.0001
p=0.3
siRNA
mock
siCOL
siPEF
(nM)
0
120
240
480
480
D
Mock
siPEF
0 min
15 min

Fig 4

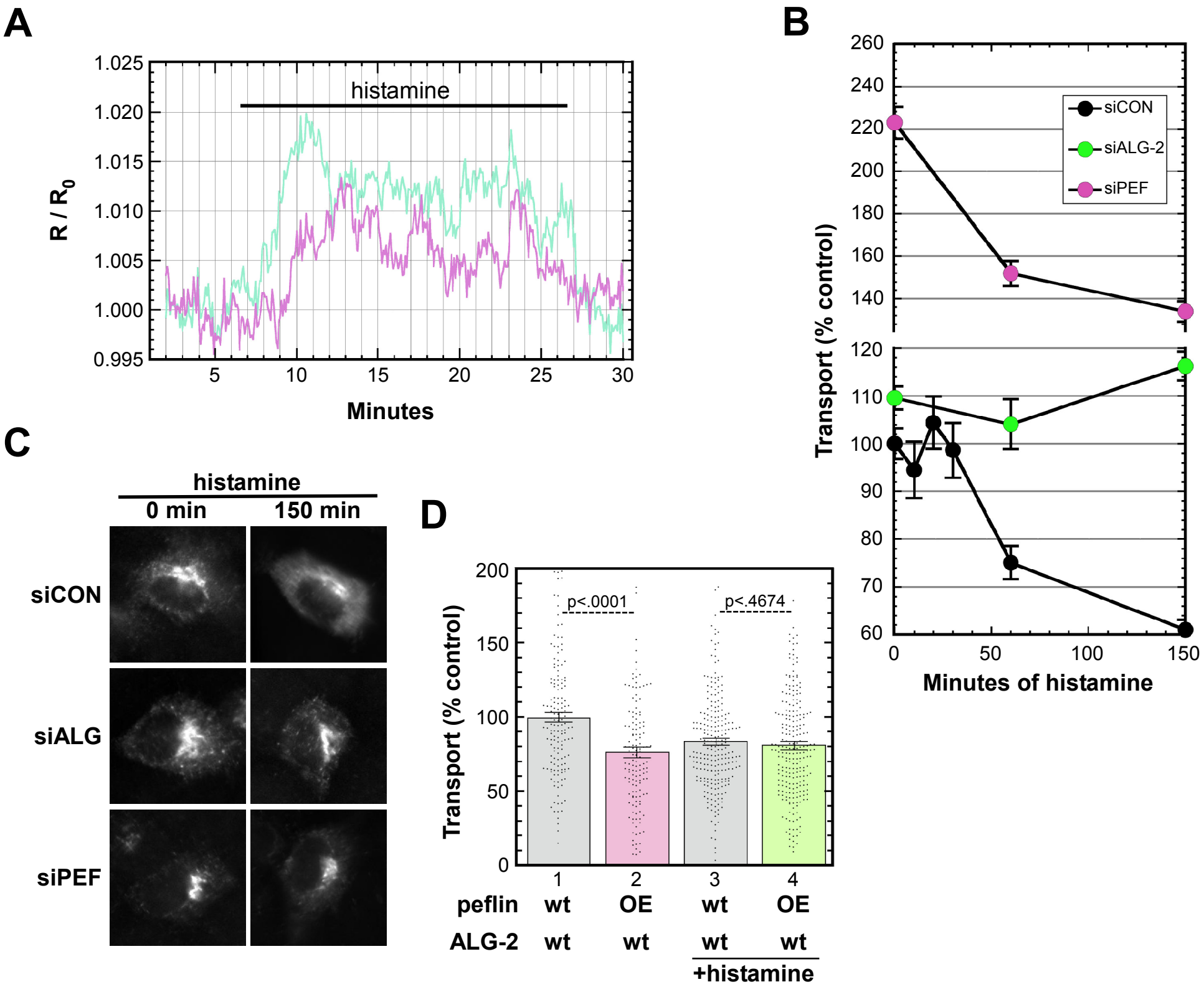
A
histamine
R / R0
Minutes
B
siCON
siALG-2
siPEF
Transport (% control)
Minutes of histamine
C
histamine
0 min
150 min
siCON
siALG
siPEF
D
p<.0001
p<.4674
Transport (% control)
peflin wt OE wt OE
ALG-2 wt wt wt wt
+histamine

Fig 5

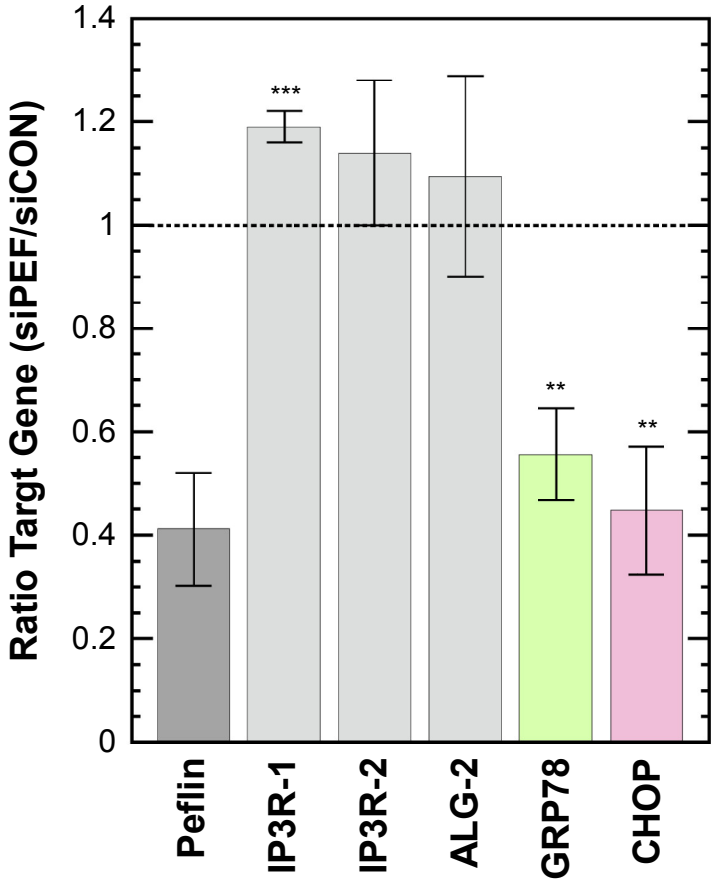
Ratio Targt Gene (siPEF/siCON)
1.4
1.2
1
0.8
0.6
0.4
0.2
0
***
**
**
Peflin
IP3R-1
IP3R-2
ALG-2
GRP78
CHOP

Fig 6